Biexcitonic four-wave-mixing signal in quantum wells: Photon-echo versus free-induction decay

H. Nickolaus and F. Henneberger
Institut für Physik, Humboldt-Universität zu Berlin, Invalidenstrasse 110, D-10115 Berlin, Germany
(Received 5 November 1997; revised manuscript received 29 December 1997)

We have performed time-integrated as well as time-resolved femtosecond degenerate four-wave-mixing measurements on inhomogeneously broadened (Zn,Cd)Se/ZnSe quantum-well structures. Potential fluctuations due to alloy disorder in the ternary wells give rise to localized quasi-zero-dimensional excitons and biexcitons. For time-integrated detection, they manifest themselves by distinct (disorder-renormalized) quantum beats. Time resolving these transients reveals a free-induction-decay-like emission nature of the biexciton in contrast to the photon-echo exciton contribution. Using a five-level scheme, containing both biexcitons and antibound two-exciton states, this striking emission-type change is explained by fluctuation and correlation effects upon the biexciton binding energy. A combination of time-resolved and time-integrated four-wave mixing is thus a powerful tool to gain information about the disorder in a given kind of quantum structure.
[S0163-1829(98)07815-1]

Disorder is an inherent feature of semiconductor quantum wells (QW's). Despite numerous works, its role in degenerate four-wave mixing (DFWM) is, however, still under debate (e.g., Refs. 1–6 and references therein). In an atomlike two-level system, inhomogeneous broadening manifests itself in a photon-echo-type signal. The DFWM transients of QW's are much more involved, as result of the complex interplay between disorder and many-body effects. Several groups[1,4–8] reported that the DFWM signal decay for linearly cross-polarized (CRP) beams is considerably faster than in the copolarized configuration (COP). Partly, this is concomitant with a change of the DFWM signal character from a photon-echo to a free-induction decay,[9,10] while other authors observe a photon echo regardless of the polarization.[5,7] It is clear that biexcitons—as the lowest-order many-body effect—are crucial for the understanding of the DFWM scenario, at least at moderate excitation.[2,11] The DFWM signal of II-VI QW's is indeed governed by pronounced biexciton features, separated by 10–15 meV from the exciton resonance.[6] This allows a clear distinction between the various processes contributing to the signal formation, and makes these structures ideal candidates for an examination of the DFWM problem.

Disorder (interface roughness, alloy fluctuations, etc.) in a QW gives rise to localization and an associated dominant inhomogeneous broadening of the optical transitions. Let Γ_X be the respective width of the exciton resonance. Localization sites of the same exciton energy E_X may vary in their biexciton binding energy Δ_B.[12] The inhomogeneous broadening of the exciton-biexciton transition ($\hbar\omega = E_X - \Delta_B$) is thus both affected by Γ_X and the width of the Δ_B fluctuation, denoted by Γ_Δ. However, an additional contribution arises from the fact that there is a correlation between Δ_B and E_X. In Fig. 1(a), we illustrate the physically more reasonable case: The stronger the localization, the larger Δ_B will be. Assuming in first order a linear relation of slope r (Ref. 12) and using Gaussian distributions for E_X and Δ_B, one obtains a width $\Gamma_B^2 = \Gamma_\Delta^2 + (1+r)^2\Gamma_X^2$ of the exciton-biexciton transition, centered at $\hbar\omega = E_X^0 - \Delta_B^0$ with E_X^0 and $\Delta_B^0 = \Delta_B^{\mathrm{QW}} + r(E_X^{\mathrm{QW}} - E_X^0)$ representing the respective average energies. In a recent study,[13] disorder of the biexciton state has been investigated by time-integrated DFWM measurements. In what follows, we demonstrate that the above-described fluctuation and correlation of the biexciton binding energy directly and crucially controls the character of the signal emission in the time domain.

The third-order response of the exciton-biexciton system in the presence of localization is appropriately treated within a five-level scheme, sketched in Fig. 1(b).[6,14] The susceptibility describing the DFWM signal then reads $\chi = \chi_X + \chi_B + \chi_A$, symbolizing the contributions from excitons (X), biexcitons (B), and antibound two-exciton states (A). The explicit expression of χ for the homogeneously broadened system is given, e.g., in Ref. 6. Averaging this susceptibility with Gaussian distributions of E_X and Δ_B yields for the relevant terms of the biexciton contribution in the time domain,

$$\chi_B(t,\tau) \propto G_B^2 \Theta(t-\tau) \exp\{-[i(E_X^0 - \Delta_B^0 - \hbar\omega) + \gamma_{XB}] \times (t-\tau)\} \exp\left\{[i(E_X^0 - \hbar\omega) - \gamma_X]\tau - \frac{\Gamma_B^2}{16\ln 2} \times (t-\tau_{\mathrm{em}})^2 - \frac{1}{16\ln 2}\left(\frac{\Gamma_X\Gamma_\Delta}{\Gamma_B}\right)^2 \tau^2\right\}, \quad (1)$$

with

$$\tau_{\mathrm{em}} = \tau(1+Q), \qquad Q = (1+r)\left(\frac{\Gamma_X}{\Gamma_B}\right)^2. \quad (2)$$

τ is the pulse delay, ω the carrier frequency, γ_X and γ_{XB} are the homogeneous widths of the exciton and exciton-biexciton transitions, respectively [for the meaning of G_B, see Fig. 1(b)]. τ_{em} defines the time where the maximum of the DFWM signal emission occurs. Figure 2 represents a plot of this time versus the biexciton parameters r and Γ_Δ/Γ_X. With no disorder of the biexciton state, a photon echo evolves ($\tau_{\mathrm{em}} = 2\tau$). For negative r, the signal emerges with

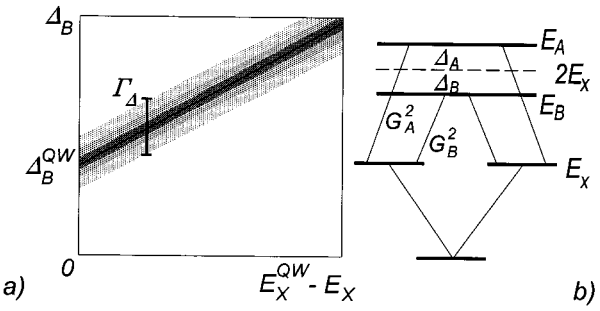

FIG. 1. (a) Variation of the biexciton binding energy in the presence of disorder. Δ_B^{QW} and E_X^{QW} are the biexciton binding and exciton energy, respectively, of the ideal QW. (b) Five-level scheme for the DFWM response of the exciton–biexciton system. $G_{B,A}^2$ are the oscillator strengths of the exciton–two-exciton transitions, normalized to the one of the single-exciton resonance.

even longer delay, while both increasing Γ_Δ/Γ_X and r make the emission more and more free-induction-like. This demonstrates that the time-resolved biexciton DFWM signal is a sensitive probe of the prevailing disorder and its character may thus change when different samples are considered. Conversely, the exciton contribution $\chi_X(t,\tau)\propto\Theta(t-\tau)\exp[-\gamma_X t - i(E_X-\hbar\omega)(t-2\tau)-\Gamma_X^2(t-2\tau)^2/16\ln 2]$ always has a photon-echo character.[6,15] The contribution from the antibound two-exciton states follows from Eq. (1), replacing Δ_B^0 by $-\Delta_A^0$ (repulsion), and using the respective broadenings (γ_{XA},Γ_A) and correlation parameter r^*. Fourier transformation of Eq. (1) provides the DFWM spectrum

$$\chi_B(\omega,\tau)\propto G_B^2\exp\left\{-\gamma_X\tau-\frac{\Gamma_X^2}{16\ln 2}\tau^2\right\}\times\exp\left\{4\ln 2\left(\frac{S}{\Gamma_B}\right)^2\right\}\mathrm{erfc}\left\{2\sqrt{\ln 2}\left(\frac{S}{\Gamma_B}\right)\right\}, \quad (3)$$

$$S=\gamma_{XB}-\frac{\Gamma_B^2 Q\tau}{8\ln 2}+i(E_X^0-\hbar\omega-\Delta_B^0). \quad (4)$$

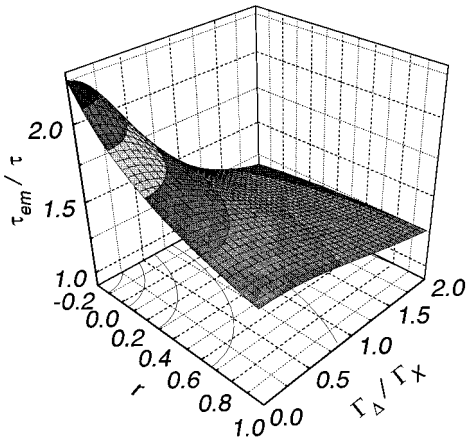

FIG. 2. Emission time τ_{em} vs the biexciton parameters r and Γ_Δ/Γ_X.

Setting $\lambda=(1+r)\Gamma_X/\Gamma_B$, Eq. (3) of Ref. 13 is recovered. Only for $r=0$ and $\Gamma_\Delta=0$, a strict photon-echo clipping spectrum follows, being typical for single excitons.[15]

Our experimental study was performed on a prototype molecular-beam-epitaxy (MBE)-grown (Zn,Cd)Se/ZnSe structure consisting of five QWs of 5-nm thickness and a Cd content of 13%, separated by 85-nm-wide ZnSe barriers. In the ternary (Zn,Cd)Se QW, alloy disorder is the main cause of localization.[12] In photoluminescence (PL), a prominent biexciton feature emerges at moderate excitation levels.[12] PL excitation and previous DFWM measurements have yielded an inhomogeneous heavy-hole exciton linewidth of $\Gamma_X=8$ meV, and an average biexciton binding energy Δ_B^0 of 11 meV, ensuring sufficiently separated exciton and biexciton resonances. The homogeneous broadening γ_X is instead on a 100 μeV scale.[6] The light-hole resonance is split off by 35 meV, and may hence be ignored in the present context. The optical pulses were provided by an optical parametric amplifier (OPA) pumped by a regenerative Ti:Sa oscillator-amplifier system, emitting 6-μJ pulses of 200-fs duration at a 200-kHz repetition rate. The polarization of the pulses was controlled by polarization filters and rotating a half-wave plate to a ratio better than 100:1. Removing the GaAs substrate by wet etching allowed measurements in forward geometry. The DFWM signal was either spectrally resolved with a monochromator, or time resolved by cross-correlating it with a reference pulse. All experiments were carried out at $T=5$ K.

The inset of Fig. 3 shows normalized DFWM spectra for $\tau=400$ fs together with the laser spectrum. In the COP case, biexcitons appear as a clear but weaker feature on the low-

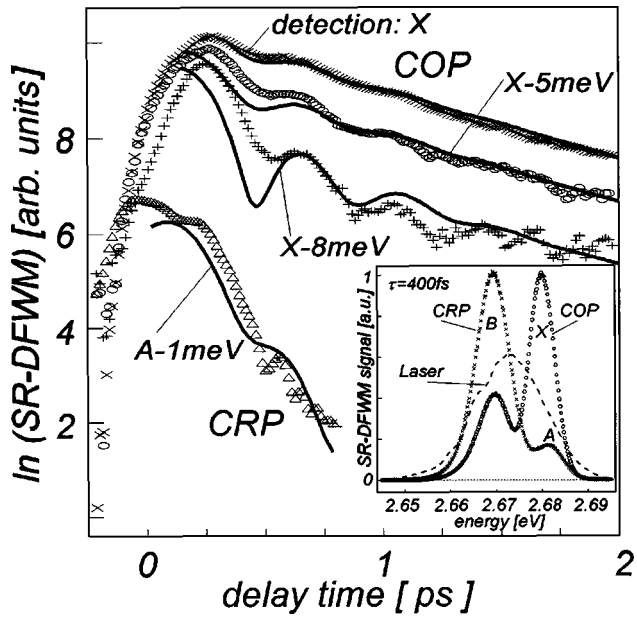

FIG. 3. Time-integrated DFWM transients for the COP and CRP cases. Dotted curves: Experiment for detection at different photon energies. Full curves: Calculations using $|\chi_X(\omega,\tau)+\chi_B(\omega,\tau)|^2$ for the COP and $|\chi_B(\omega,\tau)-\chi_A(\omega,\tau)|^2$ for the CRP configuration, respectively. Parameters: $E_x=2.68$ eV, $\Gamma_X=8$ meV, $\Gamma_B=\Gamma_A=8.8$ meV, $\Delta_B^0=11$ meV, $\Delta_A^0=1$ meV, $\gamma_X=0.5$ meV, $\gamma_{XB}=\gamma_{XA}=0$, $G_B=0.7$, $G_A=0.4$, $\Gamma_\Delta=2.7$ meV, and $r=r^*=0.05$. Inset: DFWM spectra at $\tau=400$ fs for the COP and CRP cases, respectively. Dashed line: laser spectrum.

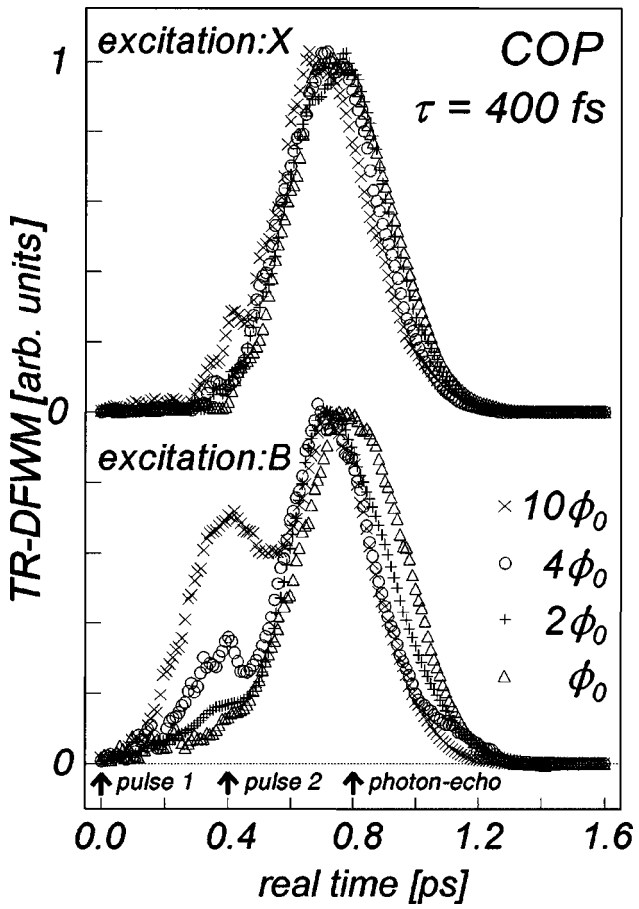

FIG. 4. Time-resolved DFWM for the COP configuration, $\tau = 400$ fs, and different densities. Upper part: Photon echo signal for excitation at the exciton. Lower part: Excitation at the biexciton transition ($\Phi_0 \approx 0.08\ \mu\mathrm{J/cm^2}$).

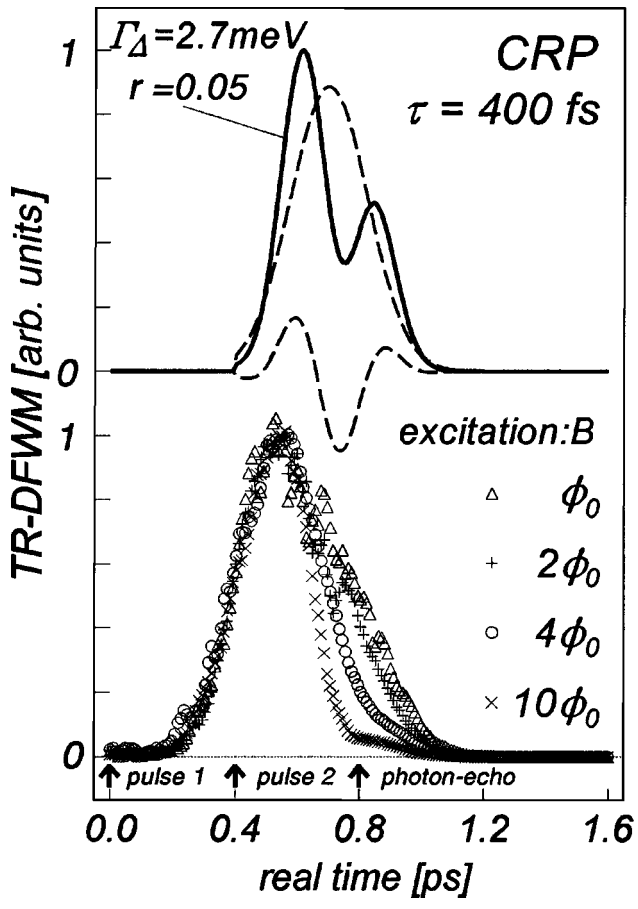

FIG. 5. Time-resolved DFWM for the CRP configuration and $\tau = 400$ fs. Lower part: Experiment for excitation at the biexciton transition and different densities. Upper part: The solid line shows the calculated signal emission using $|\chi_B(t,\tau) - \chi_A(t,\tau)|^2$ in the time domain. Parameters: see Fig. 3. The dashed lines represent $|\chi_B(t,\tau)|^2 + |\chi_A(t,\tau)|^2$ and the modulation term with period $h/(\Delta_B^0 + \Delta_A^0)$, respectively.

energy side of the exciton resonance, whereas they even dominate the spectrum in the CRP configuration. According to the relevant polarization selection rules,[6] the exciton contribution χ_X is strongly suppressed in the latter case. We therefore assign the residual high-energy feature located 1 meV above the exciton resonance to antibound two-exciton states ($\hbar\omega = E_X + \Delta_A$). For the intermediate case of COP and CRP (angle of 45° between the beam polarizations) configurations, we indeed observe a continuous high-energy shift when analyzing the DFWM signal polarization step by step.[6] This signifies clearly a change from single-exciton to two-exciton features with repulsive interaction.

In Fig. 3, the time-integrated transients for several detection energies are depicted, together with curves calculated by combining the appropriate susceptibilities from the above model. The excitation was centered at the biexciton transition. In the COP configuration, strongly damped beats occur, superimposed on the long decay of the exciton signal ($\propto |\chi_X|^2$), governed by the dephasing rate $4\gamma_X$. They are most distinct for detection between B and X. The beat frequency of 9.6 meV ($T_{\mathrm{beat}} = 430$ fs) is smaller than the separation of the DFWM peaks of $\Delta_B^0 = 11.0$ meV. This is predicted by Eq. (2), yielding an exciton-biexciton beat of frequency $Q\Delta_B^0$ ($Q \leqslant 1$), when the total COP signal $\propto |\chi_X + \chi_B|^2$ is considered. The dramatically fastened CRP decay (note the logarithmic scale) close to the exciton resonance is consistent with the occurrence of anti-bound two-exciton states with a total DFWM signal $\propto |\chi_B - \chi_A|^2$.[6] The shoulder in the CRP decay transients indicates a beat between biexciton and antibound two-exciton states of period $h/Q(\Delta_B^0 + \Delta_A^0)$. Again, the beat period of $T_{\mathrm{beat}} = 385$ fs corresponds to a somewhat smaller energy difference of 10.7 meV compared to the spectra ($\Delta_A^0 + \Delta_B^0 = 12.0$ meV). In marked contrast to the exciton contribution, the decay associated with the (either bound or antibound) two-exciton states is not controlled by a microscopic dephasing $-\gamma_{XB}$ and γ_{XA} are set to zero in the fit in Fig. 3—but by the inhomogeneous rate $\Gamma_{\mathrm{eff}} = \Gamma_X \Gamma_\Delta / \Gamma_{B,A}$.[13] In agreement with this, detecting at the biexciton maximum (not shown in Fig. 3), we observe a fast decay regardless of the polarization conditions, since the signal is here dominated by $|\chi_B|^2$.

More direct evidence of the biexciton disorder is revealed when the DFWM signal is resolved in time. The upper part of Fig. 4 shows data for excitation with COP pulses centered at the exciton transition. Indeed, a clean photon echo appears. We note that the signal duration is close to the cross correlation of the excitation pulses, and hence somewhat larger than expected from the inhomogeneous broadenings. However, when the excitation maximum is shifted to the

biexciton to pronounce this transition, an additional, free-induction-decay-like signal appears (the lower part of Fig. 4). Its distinct rise with excitation density is consistent with previous studies,[6,11] having signified an increasing contribution from biexcitons to higher-order susceptibilities. In Fig. 5, time-resolved transients for the CRP case are depicted. Here the prompt emission clearly dominates the signal. A second, much weaker signal structure occurs closer to the photon-echo time $t=2\tau$. Both features are qualitatively reproduced by the theoretical analysis presented in the upper part of Fig. 5. The beat between biexciton and antibound two-exciton states in the time-integrated CRP decay transients (lower part of Fig. 3) now gives rise to a modulation of the DFWM emission in the time domain, yielding a double structure as seen in the experiment.

In conclusion, we have both theoretically and experimentally demonstrated that disorder of the biexciton state can change the character of the DFWM emission from photon-echo to free-induction decay. It also shows up as a renormalization of the exciton-biexciton beat period. These findings might explain the partly contradictory data of different groups,[7,9] dealing obviously with QW structures of different disorder. On the other hand, DFWM turned out to be a sensitive probe, and can be utilized to diagnose the disorder in a given structure. For the present (Zn,Cd)Se QW with alloy disorder, characterized by the hierarchy $\Delta_B > \Gamma_X > \Gamma_\Delta$, the fits of the experimental data yield a biexciton binding-energy width of $\Gamma_\Delta = 2.7$ meV, and a correlation parameter $r = 0.05$. This, at first glance, somewhat surprisingly low correlation is in agreement with a previous theoretical treatment of the biexciton state with alloy disorder.[12] For a binary ZnSe QW, time-integrated data have yielded $\Gamma_X \approx \Gamma_B$ and $\Gamma_\Delta = 2.2$ meV, even resulting in a negative value for r. It will be interesting to study this correlation for structures with much stronger zero-dimensional confinement, as, e.g., quantum dots. The prompt biexciton DFWM emission in our study is not a consequence of a very large correlation r, but results from an interference between bound and antibound two-excitons, demonstrating again the substantial role of the latter, particularly for the CRP configuration. Using for these states the same disorder parameters as for the biexciton, we were able to fit the CRP transients reasonably well. Though our experimental findings are in qualitative accord with the predictions of the third-order approach, the data also signify the importance of higher-order contributions. This point deserves further investigation.

The authors thank M. Rabe for the MBE growth. This work was supported by the Deutsche Forschungsgemeinschaft by He 1939/11-1.

[1] D. Bennhardt, P. Thomas, R. Eccleston, E. J. Mayer, and J. Kuhl, Phys. Rev. B **47**, 13 485 (1993).
[2] M. Z. Maialle and L. J. Sham, Phys. Rev. Lett. **73**, 3310 (1994).
[3] T. Östreich, K. Schönhammer, and L. J. Sham, Phys. Rev. Lett. **74**, 4698 (1995).
[4] T. F. Albrecht, K. Bott, T. Meier, A. Schulze, M. Koch, S. T. Cundiff, J. Feldmann, W. Stolz, P. Thomas, S. W. Koch, and E. O. Göbel, Phys. Rev. B **54**, 4436 (1996).
[5] G. Bongiovanni, S. Gürtler, A. Mura, F. Quochi, and J. L. Staehli, Semicond. Sci. Technol. **12**, 300 (1997).
[6] T. Häupl, H. Nickolaus, F. Henneberger, and A. Schülzgen, Phys. Status Solidi B **194**, 219 (1996).
[7] T. Saiki, M. Kuwata-Gonokami, T. Matsusue, and H. Sakaki, Phys. Rev. B **49**, 7817 (1993).
[8] S. Adachi, T. Miyashita, S. Takeyama, Y. Takagi, A. Takeuchi, and M. Nakayama, Phys. Rev. B **55**, 1654 (1997).
[9] S. T. Cundiff, H. Wang, and D. G. Steel, Phys. Rev. B **46**, 7248 (1992).
[10] H. H. Yaffe, Y. Prior, J. P. Harbinson, and L. T. Florez, J. Opt. Soc. Am. B **10**, 578 (1993).
[11] G. Bartels, V. M. Axt, K. Victor, A. Stahl, P. Leisching, and K. Köhler, Phys. Rev. B **51**, R11 217 (1995).
[12] J. Puls, H.-J. Wünsche, and F. Henneberger, Chem. Phys. **210**, 235 (1996).
[13] W. Langbein, J. M. Hvam, M. Umlauff, H. Kalt, B. Jobst, and D. Hommel, Phys. Rev. B **55**, R7383 (1997).
[14] F. Kreller, M. Lowisch, J. Puls, and F. Henneberger, Phys. Rev. Lett. **75**, 2420 (1995).
[15] J. Erland, K.-H. Pantke, V. Mizeikis, V. G. Lyssenko, and J. M. Hvam, Phys. Rev. B **50**, 15 047 (1994).